SUPPORTING INFORMATION:

Thorough multianalytical characterization and quantification of micro-and nanoplastics from Bracciano Lake's sediments

Andrea Corti [1], Virginia Vinciguerra [1], Valentina Iannilli [2], Loris Pietrelli [2], Antonella Manariti [1], Sabrina bianchi [1], Antonella Petri [1], Mario Cifelli [1], Valentina Domenici [1], Valter Castelvetro [1]*

[1] Dipartimento di Chimica e Chimica Industriale, via Moruzzi 13, 56126 Pisa (Italy); (AC: andrea.corti@unipi.it; VV: virgi-vinci@hotmail.it; SB: sabrina.bianchi@unipi.it; AP: antonella.petri@unipi.it; AM: antonella.manariti@ unipi.it; MC: mario.cifelli@unipi.it; VD: valentina.domenici@unipi.it)

[2] ENEA Casaccia, Via Anguillarese, 301, 00123 Rome (Italy); (VI: valentina.iannilli@enea.it; LP: loris.pietrelli@enea.it)

* Correspondence: valter.castelvetro@unipi.it.

S1. ATR-FTIR analysis of plastic fragments collected as the sieve fraction between 2 and 5 mm

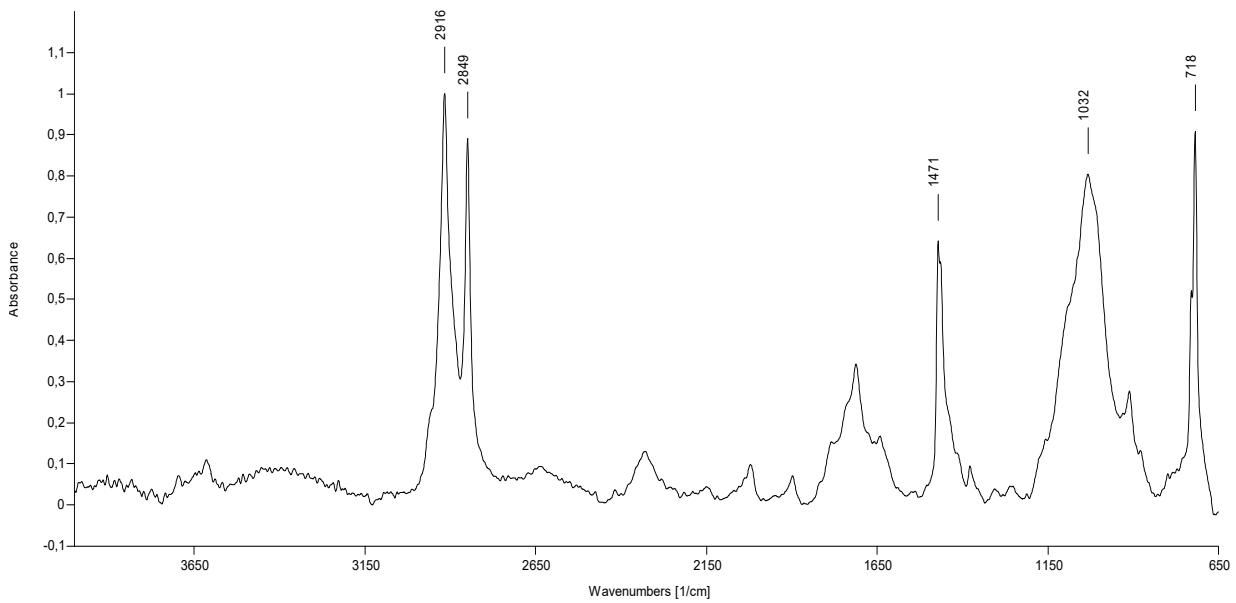

Figure SI1. ATR spectrum of the BR1B3-f_1 fragment.

Table SI1. Characteristic IR absorptions of polyethylene (compare with figure SI1)

Wavenumber (cm^{-1})		Vibrational mode
Theoretical	**Observed (BR1B3-f_1)**	
2915, 2845	2916, 2849	ν_s CH
1472, 1462	1471	δ_s CH_2
730, 717	718	ρ CH_2

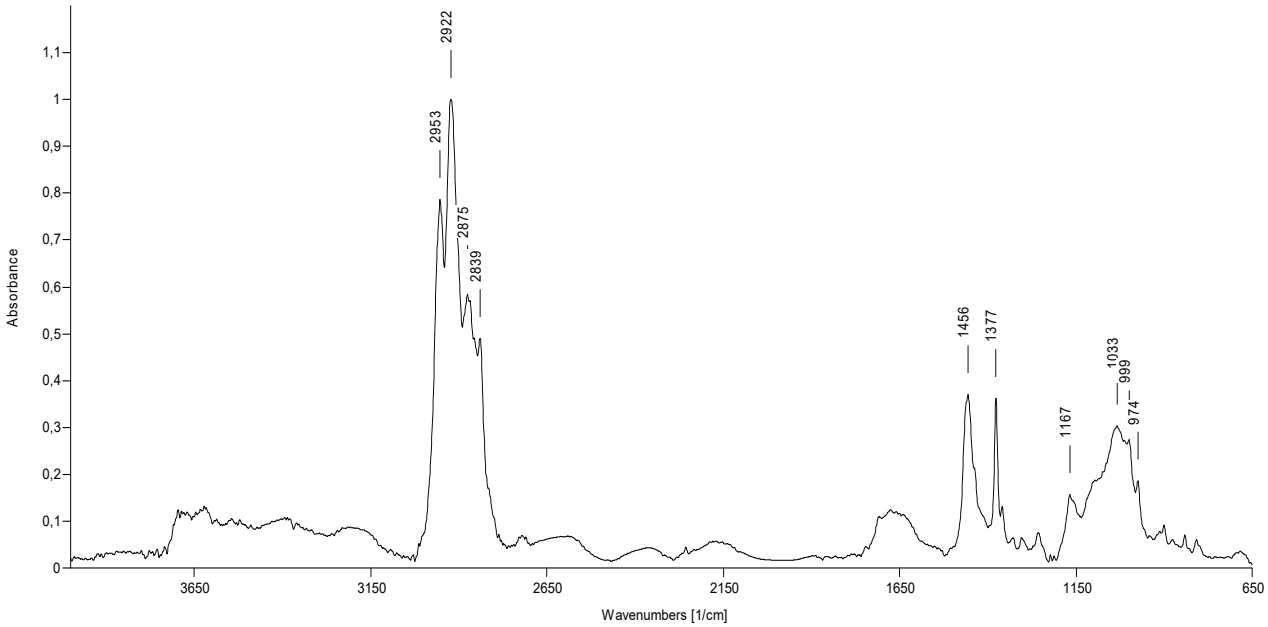

Figure SI2. ATR spectrum of the BR2C2-f_3 fragment.

Table SI2. Characteristic IR absorptions of polypropylene(compare with figure SI2)

Wavenumber (cm^{-1})		**Vibrational mode**
Theoretical	**Observed (BR2C2-f_3)**	
2950, 2915, 2838	2953, 2922, 2875, 2839	ν_s CH
1455	1456	δ_s CH_2
1377	1377	δ_s CH_3
1166	1167	δ_s CH, ρ CH_3, ν_s C-C
997	999	ρ CH_3, δ_s CH_3, δ_s CH
972	974	ρ CH_3, ν_s C-C
840	841	ρ CH_2, ν_s C-CH_3
808	809	ρ CH_2, ν_s C-C, ν_s C-CH

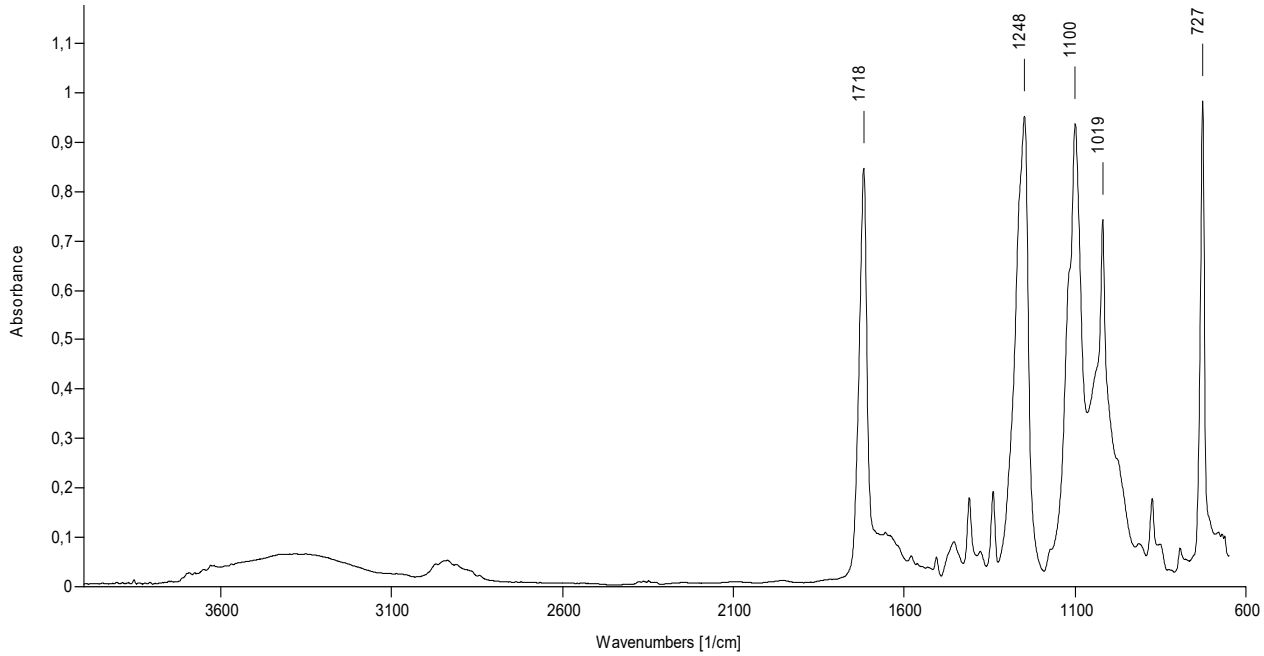

Figure SI3. ATR spectrum of the BR2B2-f_1 fragment.

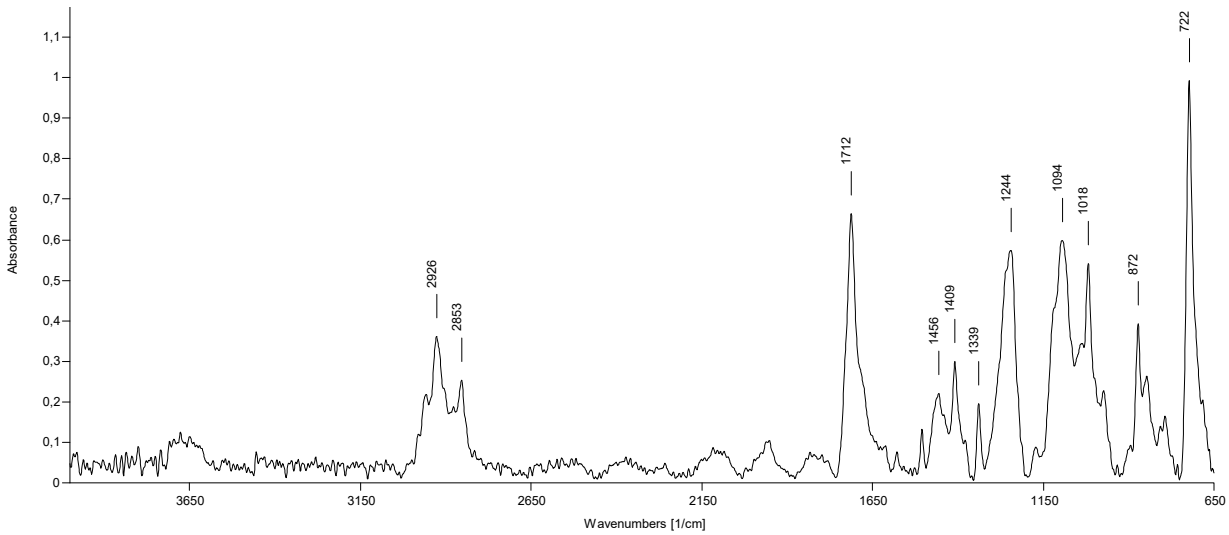

Figure SI41. ATR spectrum of the BR2C2-f_1 fragment.

Table SI3. Characteristic IR absorptions of polyethylene terephthalate (compare with figure SI3 and SI4)

Wavenumber (cm^{-1})		Vibrational mode
Theoretical	**Observed (BR2B2-f_1 and BR2C2-f_1)**	
2925, 2850	2926, 2853	ν_{as} and ν_s of CH_2
1720	1718-1712	ν_s C=O
1250	1248-1244	ν_s C(=O)-O
1175	1173 (weak)	1,4-disubstituted ring C-C stretching
1120	1118 (shoulder)	ν_s C-O, trans-conformer
1020	1018-1019	1,4-disubstituted ring C-C stretching
870	872	ring C-C stretching
730	722-727	$\delta_{out\text{-}of\text{-}plane}$ of ring C-H and ester C=O

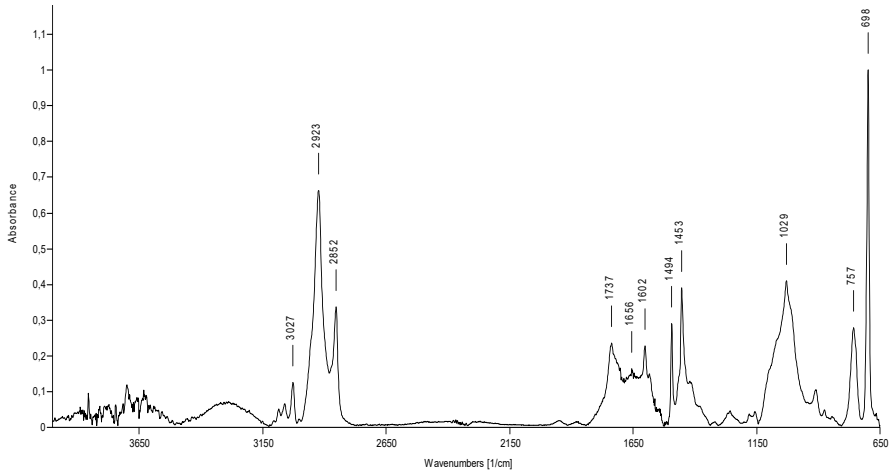

Figure SI5. ATR spectrum of the BR1C3-f_2 fragment.

Table SI4. Characteristic IR absorptions of polystyrene (compare with figure SI5)

Wavenumber (cm^{-1})		Vibrational mode
Theoretical	**Observed (BR1C3-f_2)**	
3024	3027	ν_s aromatic CH
2847	2852	ν_s CH
1601, 1492	1602, 1494	ν_s aromatic ring
1451	1453	δ_s CH_2
1027	1029	δ_s aromatic CH
694	698	δ_s aromatic CH out of plane

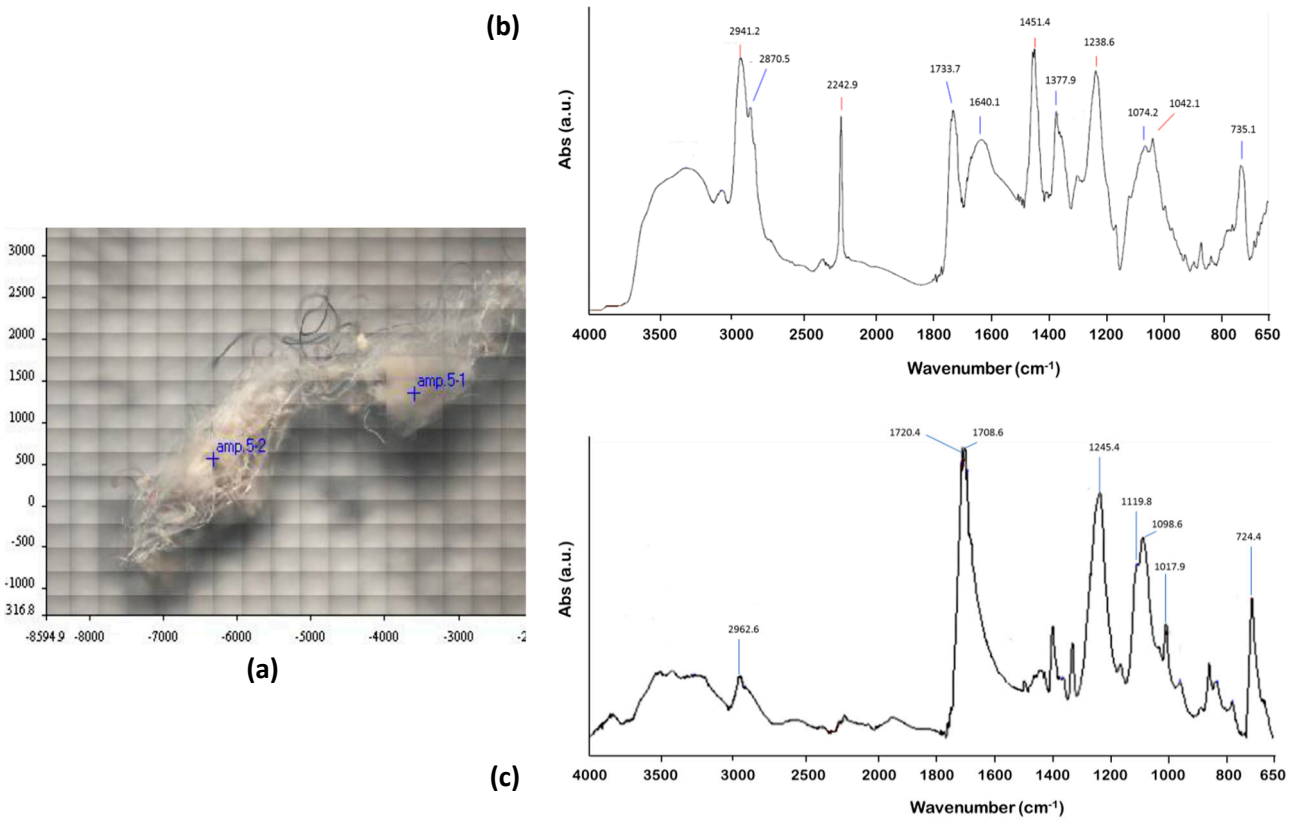

Figure SI6. **a)** Optical microscopy image showing the spots of the surface of fragment BR1C3-f_4 analysed by micro-ATR; **b)** micro-ATR FTIR of spot 5-1 (isolated black fiber); **c)** micro-ATR FTIR of spot 5-2 (white fibers).

The spectra reported in **Figure SI6** indicate that the aggregate of microfibers is based on PET (spectrum SI6-c) the most common synthetic polyester textile fiber (as reported in **Table SI3**.) and on a minor amount of acrylic fibers (spectrum SI6-b), as shown by the nitrile peak at 2242.9 cm^{-1} typical of acrylonitrile copolymers.

S2. ATR analysis of natural and plastic fragments isolated in the passing fraction (size < 2 mm)

In **Figure SI7(b)** the peaks at 1411, 843, and 711 cm^{-1} can be assigned to calcium carbonate. In addition, the absorption bands at 3289 cm^{-1} (O-H and/or N-H stretching modes), 1656 and 1536 cm^{-1} (Amide-I N-C=O stretching and Amide-II N-H deformation) are attributable to proteins, such as conchiolin in natural sea shell. Thus, the spectrum may be assigned to sea shell.

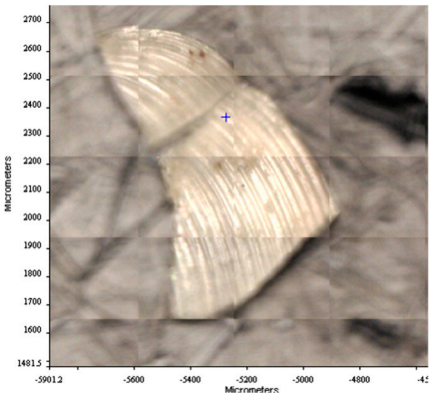

(a)

(b)

Figure SI7. Biogenic fragment from BR1C3: **a)** optical microscopy image; **b)** micro-ATR FTIR.

S3-Spectroscopic analysis of dichloromethane-extractable fractions

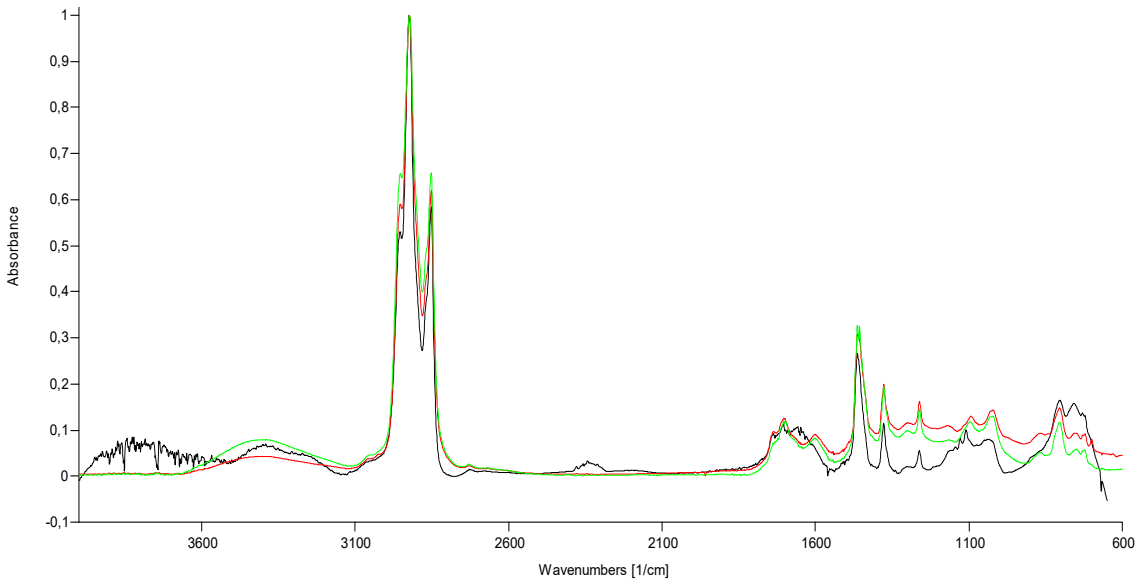

Figure SI8. FT-IR spectra of BR1A1 (green line), BR1B1 (red line) and BR1C1 (black line) extracts in CH_2Cl_2.

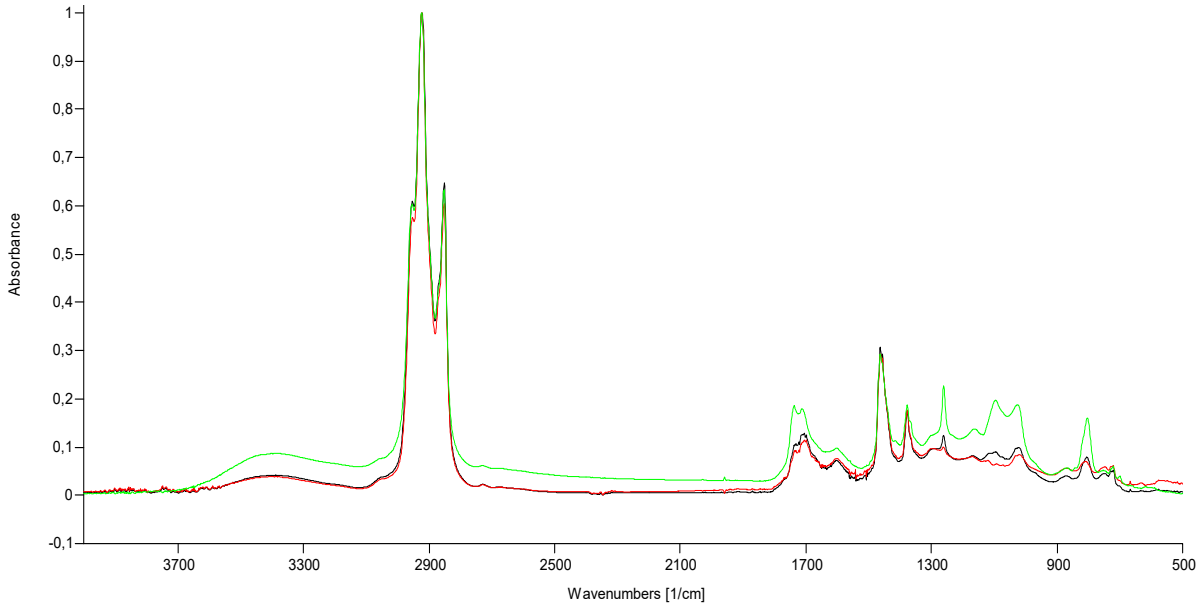

Figure SI9. FT-IR spectra of BR1A2 (red line), BR1B2 (black line) and BR1C2 (green line) extracts in dichloromethane.

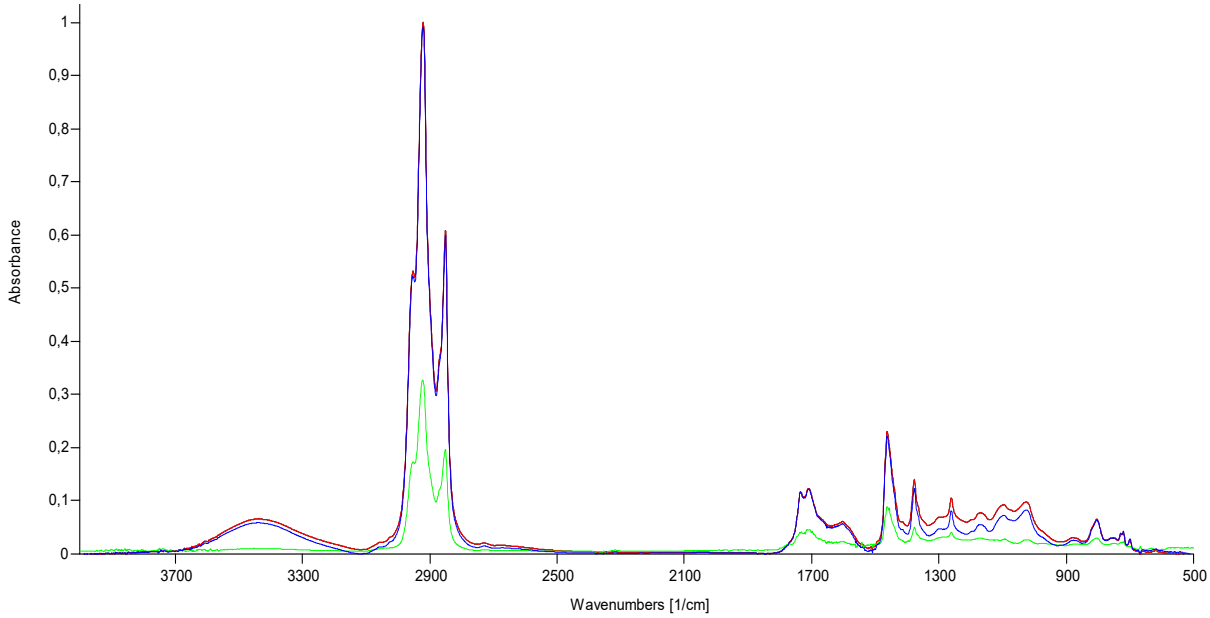

Figure SI10. FT-IR spectra of BR1A3 (red line) and BR1B3 (blue line) and BR1C3 (green line) extracts in dichloromethane.

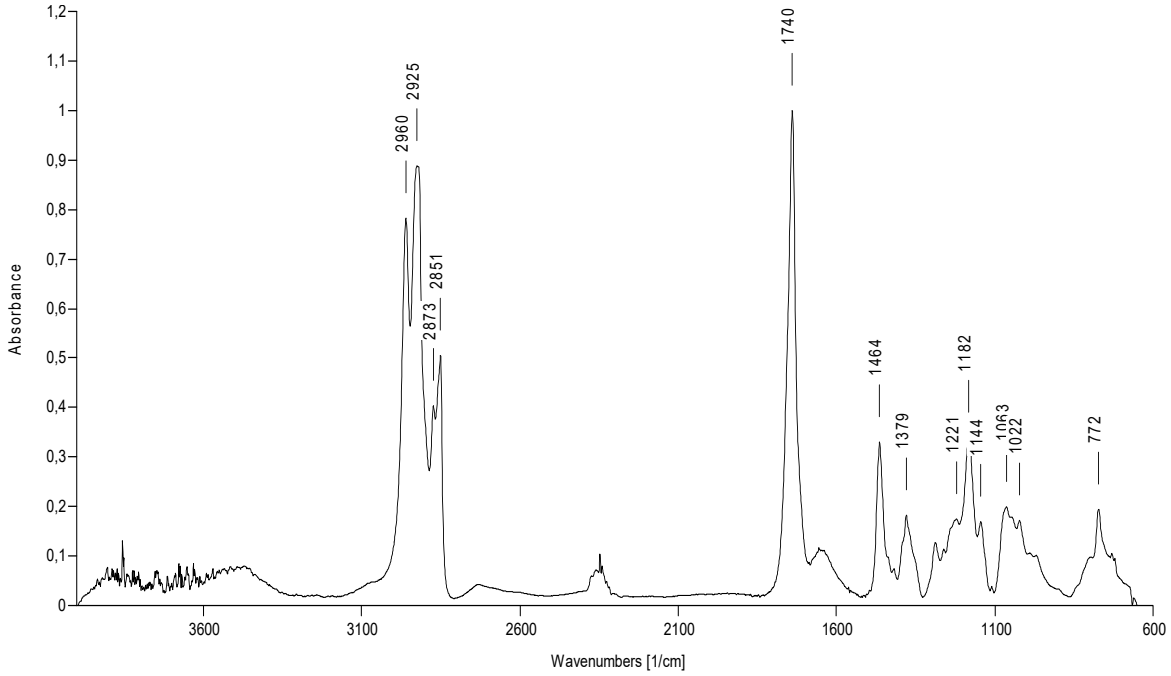

Figure SI11. FT-IR spectrum of the BR2B3 sample extracted in in dichloromethane

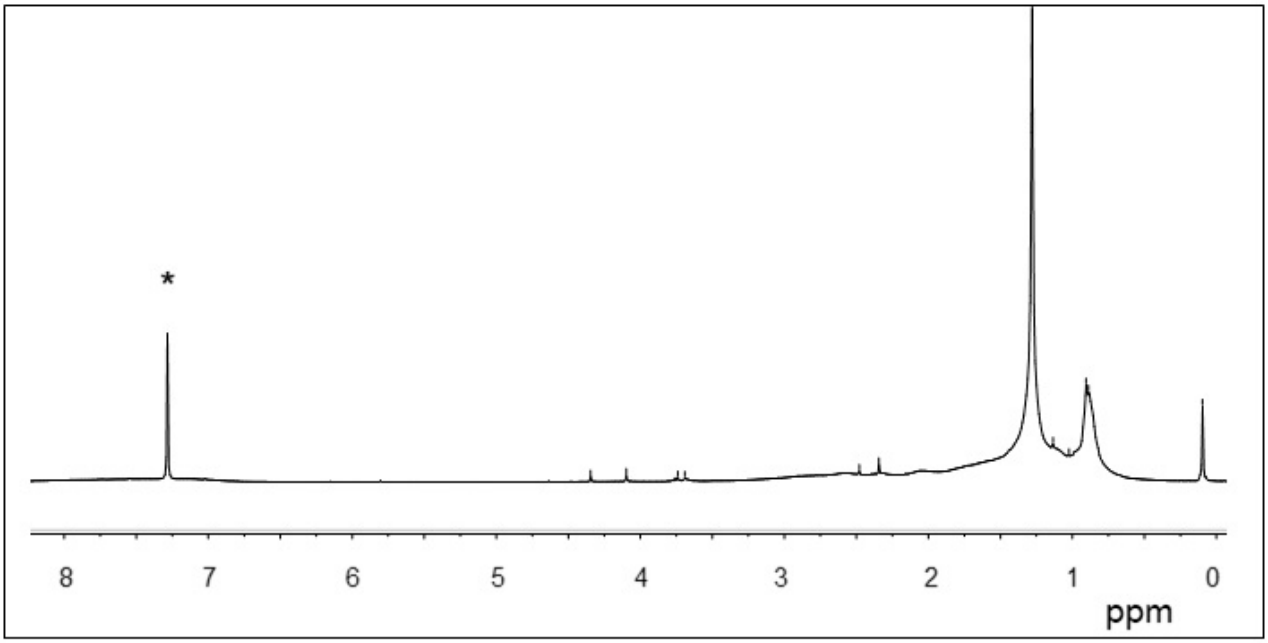

Figure SI12. ^{1}H-NMR spectrum of the BR1B1 sample extracted in dichloromethane.

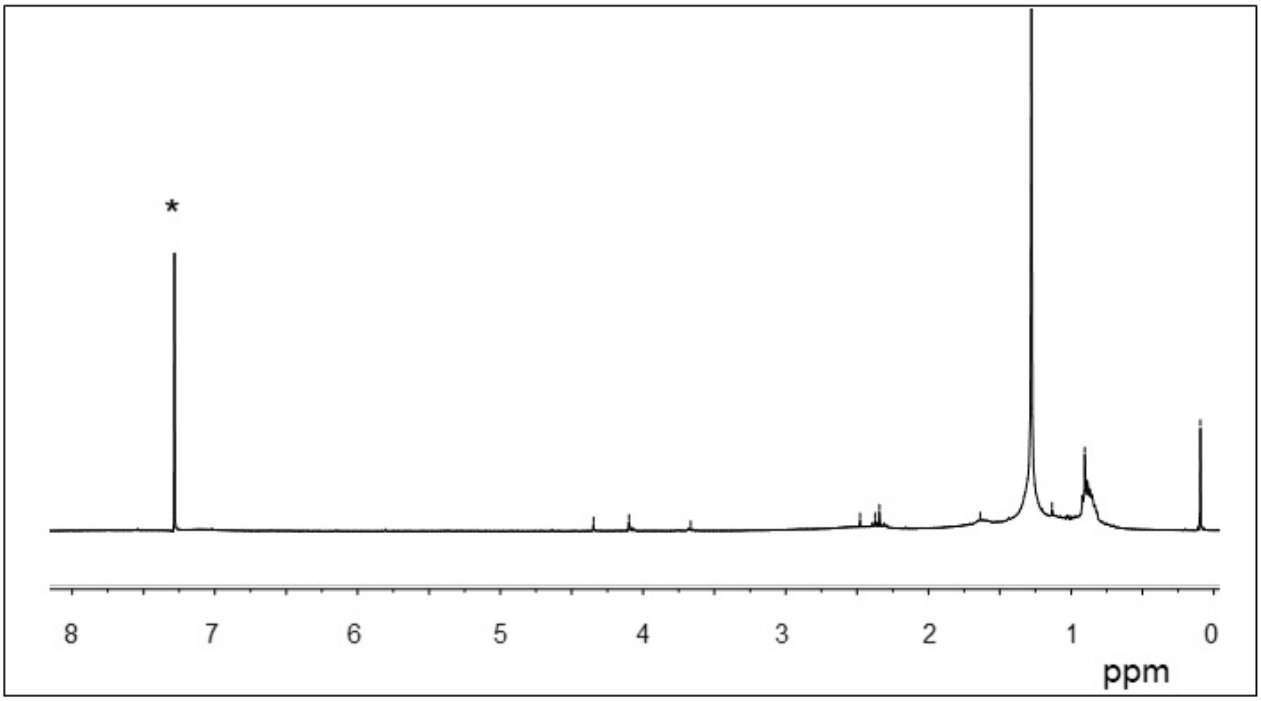

Figure SI13. ^{1}H-NMR spectrum of the BR1C3 sample extracted in dichloromethane.

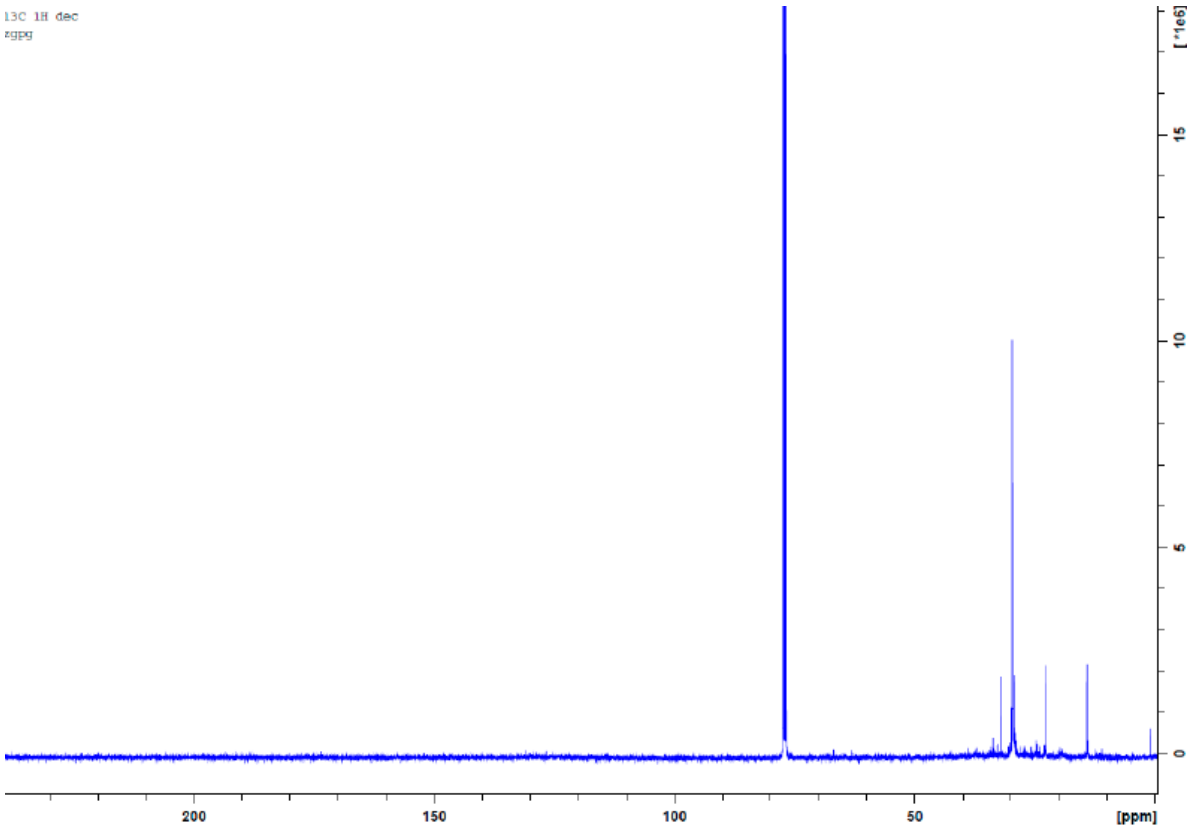

Figure SI14. ^{13}C-NMR spectrum of the BR1B3 sample extracted in dichloromethane.

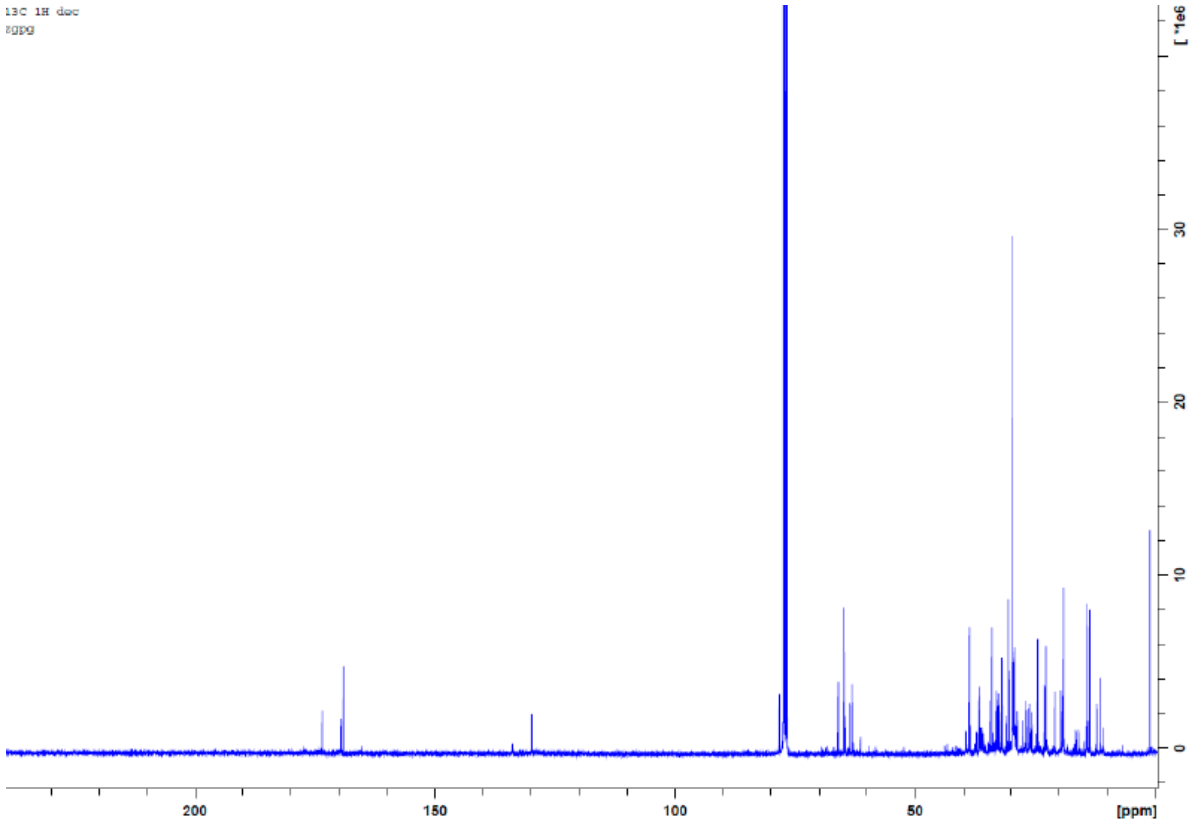

Figure SI15. ^{13}C-NMR spectrum of the BR2B3 sample extracted in dichloromethane.

S4. Analysis of DCM extracts by Size Exclusion Chromatography (SEC)

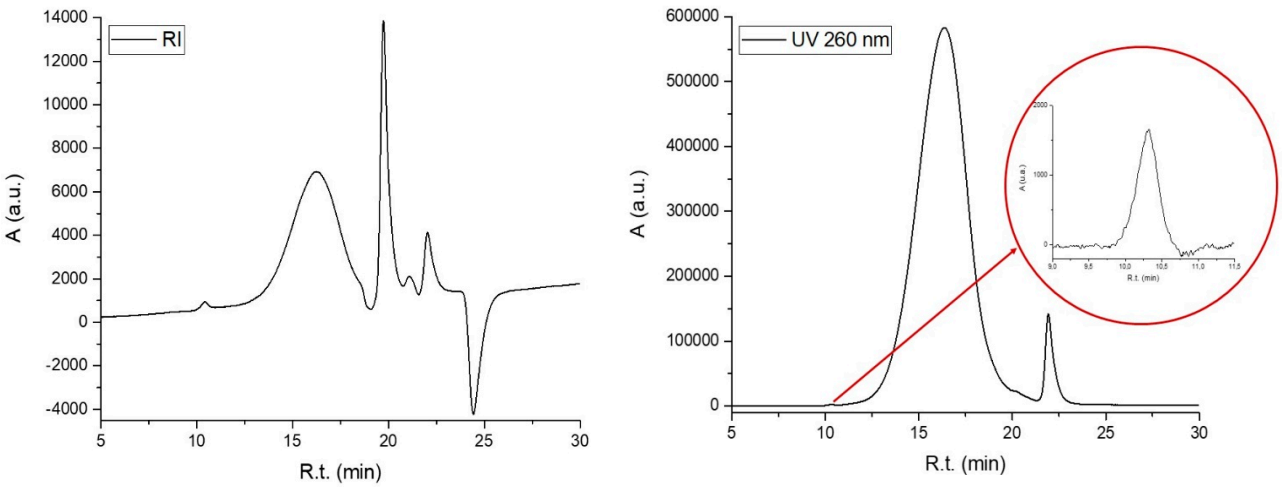

(a) **(b)**

Figure SI16. SEC profiles as recorded by **(a)** Refractive index and **(b)** UV (λ=260 nm) detectors from DCM extracts of BR1A1 sample.

Figure SI17 shows the linear interpolation of the experimental data obtained by injecting three replicates of containing 0.5-4.5 mg / ml of PS dissolved in chloroform; the injection volume in the column is 50 µL.

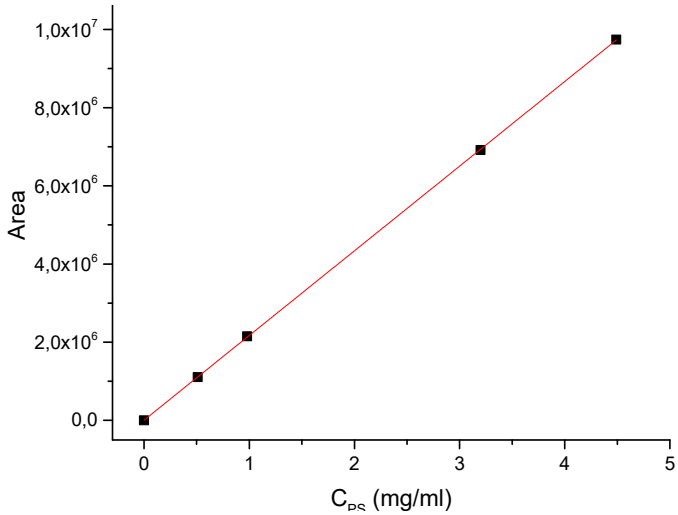

Figure SI17. Calibration line recorded with UV detector (260 nm) for SEC analysis.

Equation line: $A = 2.17E + 6 * C + 6033.36$ r^2=0.99998

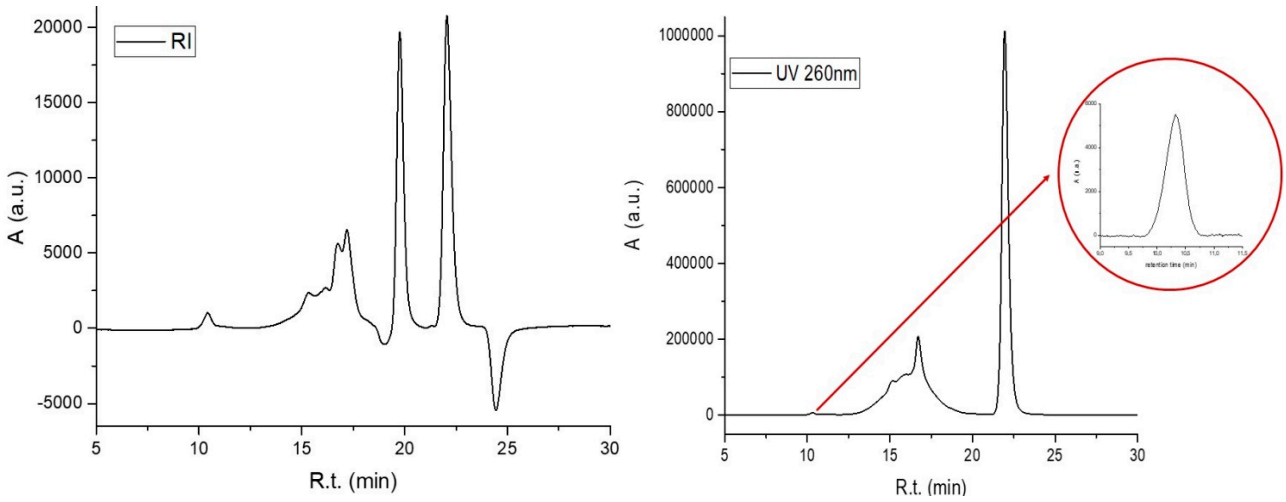

(a) **(b)**

Figure SI18. SEC profiles as recorded by **(a)** Refractive index, and **(b)** UV (λ=260 nm) detectors from DCM extracts of BR2A2 sample.

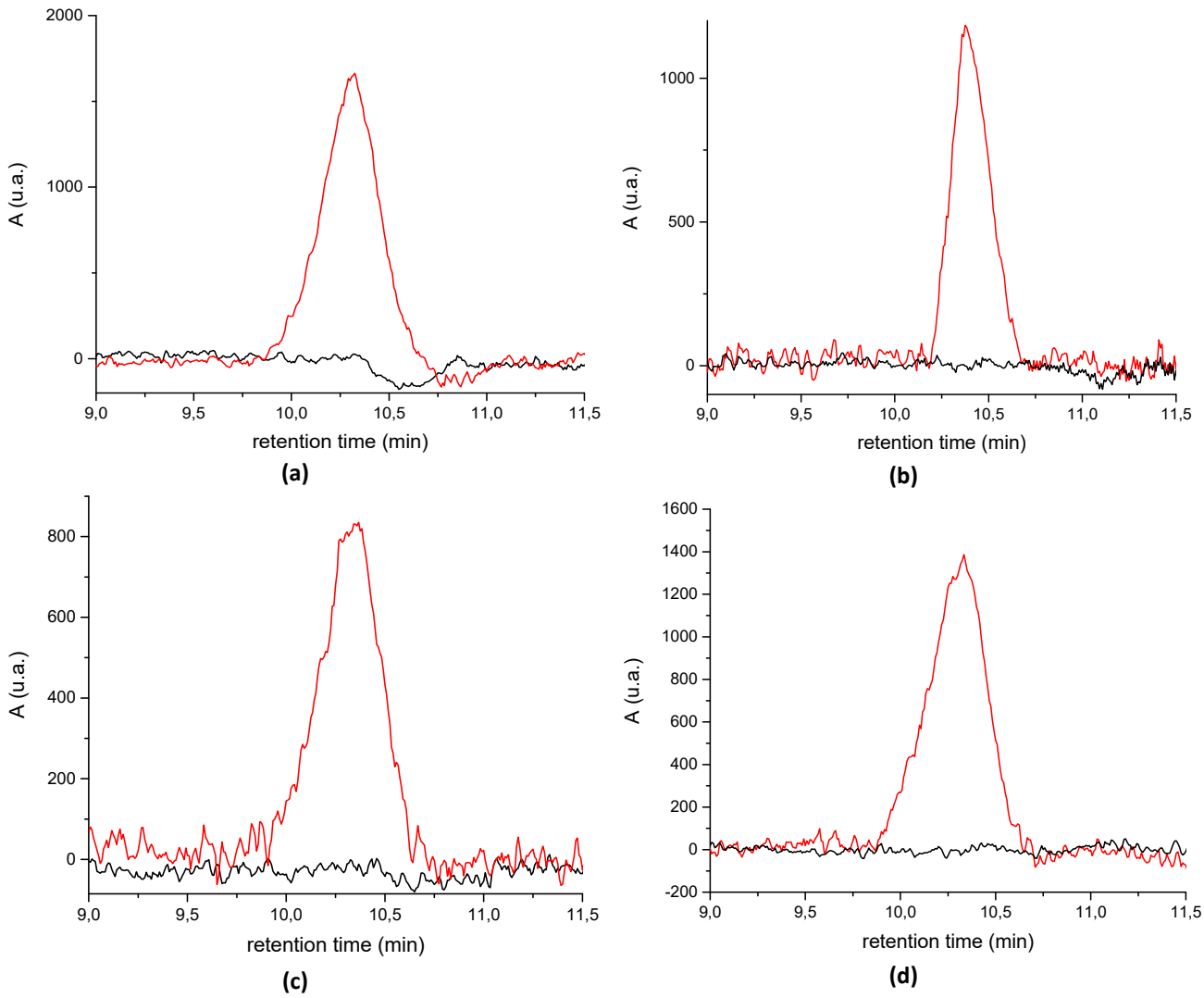

Figure SI19. UV 260 nm (red line) and UV 340 nm (black line) SEC profiles of DCM extracts from: a) BR1A1; b) BR1B3; c) BR2A3; d) BR2C2.

S5. Calibration for HPLC analysis

Figure SI20 shows the linear interpolation of the experimental data obtained by injecting three replicates of containing 1.25, 2.5, 5 and 9 mg/L of dissolved TPA in NaOH solution submitted to the sample pre-treatment procedure; the injection volume in the column is 50 µL.

(a) **(b)**

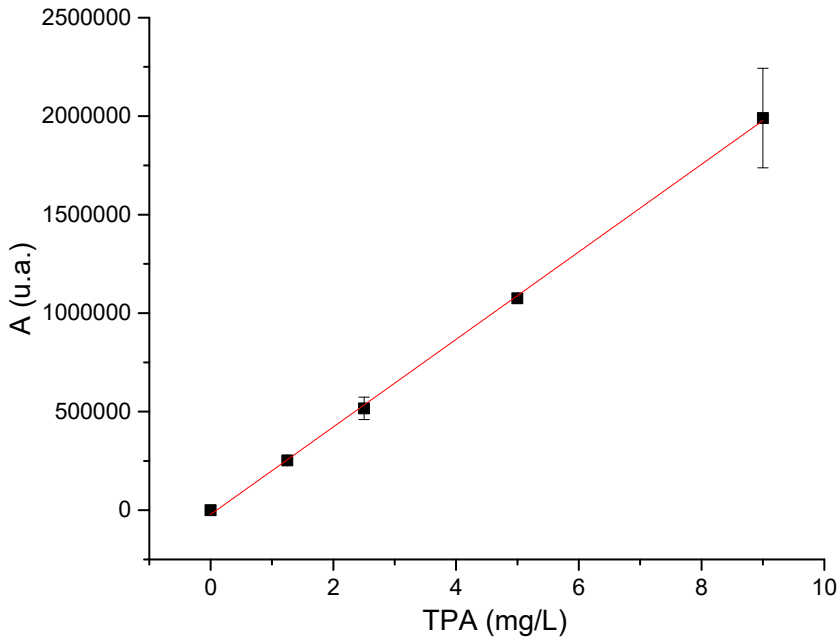

Figure SI20. Experimental calibration line for HPLC quantitative analysis of TPA

Equation line: $A = 2.21E + 8 * C - 21633.7$ r^2=0.9998

LOD: 136 µg/kg LOQ:453 µg/kg

LOD and LOQ have been calculated as following:

$$LOD = \left(\frac{\sigma_{sol.A}}{m_{line}} * 3\right) * 10^6 \qquad LOQ = \left(\frac{\sigma_{sol.A}}{m_{line}} * 10\right) * 10^6$$

where "$\sigma_{sol.}A$" is the standard deviation relevant to the absorbance recorded from multiple injections of the most diluted solutions (1.25 mg/L) of the calibration curve and "m line" is the slope of the calibration curves; 0.05 % probability level for false positive decisions was considered.